Biochimica et Biophysica Acta 1818 (2012) 1410–1419

Contents lists available at SciVerse ScienceDirect

Biochimica et Biophysica Acta

journal homepage: www.elsevier.com/locate/bbamem

# Ethanol perturbs lipid organization in models of stratum corneum membranes: An investigation combining differential scanning calorimetry, infrared and $^{2}$H NMR spectroscopy

Sungjong Kwak [a], Elana Brief [b], Denis Langlais [b], Neil Kitson [d], Michel Lafleur [a,*], Jenifer Thewalt [b,c,d,**]

[a] Department of Chemistry, Center for Self-Assembled Chemical Structures (CSACS), Université de Montréal, C.P. 6128, Succ. Centre Ville, Montréal, Québec, Canada H3C 3J7
[b] Department of Physics, Simon Fraser University, Burnaby, British Columbia, V5A 1S6, Canada
[c] Department of Molecular Biology and Biochemistry, Simon Fraser University, Burnaby, British Columbia, Canada V5A 1S6
[d] Department of Dermatology and Skin Science, University of British Columbia, Vancouver, British Columbia, Canada V5Z 4E8

ARTICLE INFO

*Article history:*
Received 2 December 2011
Received in revised form 3 February 2012
Accepted 10 February 2012
Available online 16 February 2012

*Keywords:*
Ethanol
$^{2}$H NMR
IR
DSC
Ceramide
Stratum corneum

ABSTRACT

Ethanol is used in a variety of topical products. It is known to enhance the permeability of the skin by altering the ability of the stratum corneum (SC) intercellular membranes to form an effective barrier. In addition, ethanol and other alcohols are key components of antiseptic gels currently used for hand wash. Using infrared and deuterium NMR spectroscopy as well as calorimetry, we have investigated the effect of ethanol on a model membrane composed of lipids representing the three classes of SC lipids, an equimolar mixture of N-palmitoylsphingosine (ceramide), palmitic acid and cholesterol. Ethanol is found to influence the membrane in a dose dependent manner, disrupting packing and increasing lipid motion at low concentrations and selectively extracting lipids at moderate concentrations.



## 1. Introduction

The stratum corneum (SC) is the outer layer of mammalian skin, a terminally differentiated epithelium that provides the essential barrier between the environment and the interior milieu. For practical biological purposes, it is waterproof. The tissue consists of impermeable fully differentiated epithelial cells ("corneocytes") connected by a network of intercellular junctions ("corneodesmosomes") and immersed in stacks of unusual biological membranes ("stratum corneum intercellular membranes"). These membranes are thought to be the rate limiting step in, for example, the transdermal passive diffusion of water, and the most probable route for diffusion of drugs and toxins through the skin [1–3]. Predicting and modifying such diffusion is a subject of intense research and debate.

Our particular interest is the relationship between lipid composition and membrane structure, and as a consequence, the nature of membrane function, and in particular permeability. The unusual lipid composition of SC (approximately equimolar amounts of ceramide, cholesterol, and saturated free fatty acid) is related to its unusual structure (solid crystalline lipid domains and asymmetric bilayer stacking) and this suggests to us the significance of *in vivo* molecular self-organization. In previous work, the phase behavior of an equimolar mixture of *N*-palmitoyl D-*erythro*-sphingosine (Cer16), palmitic acid (PA), and cholesterol (chol) was investigated [4]. Cer16 is a non-hydroxyl ceramide bearing a hexadecanoyl chain. For this model mixture, we selected representatives of the three main lipid classes of SC intercellular membranes that would be optimized for hydrophobic matching. Despite this molecular feature that should promote lipid mixing, it was found that the mixture demonstrated extensive phase separation and, at physiological temperature, spontaneously formed lipid dispersions mainly consisting of solid lipid crystals with orthorhombic chain packing, analogous to natural SC lipids [5–10]. This mixture underwent a solid-to-fluid phase transition above 45 °C, a feature also reminiscent of the observed thermal behavior of extracted SC lipids [11–13]. Study of individual lipid species in such dispersions revealed that their thermotropic behavior was not identical. The initial part of the transition involved the formation of a liquid ordered (lo) phase that contained mainly PA and cholesterol, with a limited amount of Cer16. Subsequent heating led to the progressive solubilization of Cer16 into the fluid lamellar phase. It is inferred that the components of the SC lipid fraction do not respond equally when the mixture stability is challenged with heat.

*Abbreviations:* SC, Stratum corneum; Cer16, *N*-palmitoyl D-*erythro*-sphingosine; PA, palmitic acid; chol, cholesterol; lo, liquid ordered; Cer16-$d_{31}$, *N*-perdeuterated-palmitoyl D-*erythro*-sphingosine; PA-$d_{31}$, perdeuterated palmitic acid

* Corresponding author. Fax: +1 514 343 7586.
** Correspondence to: J. Thewalt, Department of Physics, Simon Fraser University, Burnaby, British Columbia, Canada V5A 1S6. Fax: +1 604 291 3592.
*E-mail addresses:* michel.lafleur@umontreal.ca (M. Lafleur), jthewalt@sfu.ca (J. Thewalt).

0005-2736/$ – see front matter © 2012 Elsevier B.V. All rights reserved.
doi:10.1016/j.bbamem.2012.02.013

From this perspective we wondered whether different lipid components would be likewise differentially affected by organic solvents, particularly ethanol (EtOH). EtOH is commonly employed as a "permeability enhancer" for transdermal drugs as it is well known for its ability to increase skin permeability. SC permeation by EtOH is associated with the alcohol content in the binary EtOH/$H_2O$ system. It was found that, for several different chemicals, the optimal range of EtOH was between 40 and 80 (v/v)% [14–20], smaller and larger proportions of EtOH in water showing more limited penetration enhancing effect. The enhanced permeation observed in the presence of EtOH was proposed to be associated with different mechanisms including the fluidification of the intercellular lipid matrix [14,21], the extraction of epidermal lipidic components [17,19,21–24], the alteration of SC keratin protein conformation [17,21], a "pull effect" that involves co-permeation of the drug and the alcohol [18,20,25,26] and an increase of the drug's solubility in the SC (that could be associated with membrane fluidification and/or the pull effect) [15,18,27]. The relative efficacy of these mechanisms is believed to be dependent on the proportion of EtOH as well as the nature of the drug, and EtOH-induced increased drug absorption for a given system may be due to more than one mechanism.

Another relevant aspect of this work is associated with the current use of EtOH-based gels as an antiseptic, particularly for human hands. These products, widely available, have an alcohol (EtOH or other alcohols) content of about 60%. Even though the immediate goal of disinfection is fulfilled by these gels, little attention has been devoted to studying potential unexpected effects of the repetitive exposure to these EtOH-based gels on the integrity of the skin barrier.

The results reported here show that increasing concentrations of EtOH in aqueous dispersions of our model lipid membranes indeed had diverse effects on component ceramides and free fatty acids. The use of synthetic lipids allowed us to make mirror mixtures in which the phase behavior of each specific component could be examined. Despite the fact that it is a rather crude SC lipid model, the Cer16/PA/chol equimolar mixture presents the considerable advantage of providing an unambiguous identification of the SC lipid constituents which are more susceptible to EtOH. Consequently, studying this simple mixture allows us to identify EtOH/lipid interactions that are likely to influence SC permeation.

## 2. Materials and methods

Both synthetic *N*-palmitoyl D-*erythro*-sphingosine (Cer16), and the perdeuterated ceramide analogue (Cer16-$d_{31}$) were purchased from Northern Lipids Inc. (Vancouver, BC). PA and cholesterol were acquired from Sigma Chemical Co. (St. Louis, MO). Perdeuterated palmitic acid (PA-$d_{31}$) was obtained from CDN Isotopes (Pointe-Claire, Québec) for all experiments except the $^2$H-NMR work which used PA-$d_{31}$ resulting from the deuteration of PA [28]. HPLC grade ethanol was purchased from Aldrich (Milwaukee, WI).

### 2.1. DSC

Equimolar quantities of Cer16, PA-$d_{31}$, and Chol were weighed, mixed together co-dissolved in benzene/methanol, 95:5 (v/v) and freeze-dried. The lipid powder was transferred into a capillary tube and was hydrated with a large excess of 2-[*N*-morpholino] ethanesulfonic acid (MES) buffer (100 mM MES, 100 mM NaCl, and 5 mM EDTA), pH 5.4. For samples containing EtOH, premixed EtOH/MES buffer solution was added for hydrating the lipid powder. The EtOH proportions are expressed in (v/v)%. The tubes were then flame-sealed to prevent the evaporation of the buffer and EtOH. The solid lipid weight was between 1 and 2 mg, and about 4 to 5 μL of buffer or EtOH/buffer solutions were added. The samples underwent a freeze-thaw procedure. The samples were heated to ~95 °C for 10 min. This heating period was followed by cooling the sample in liquid nitrogen. This cycle was repeated three times. Lipid mixtures of this type are very sensitive to their thermal history [29,30] thus a systematic equilibration procedure was imposed on all of the samples. After being hydrated, the samples were kept at 40 °C for two weeks, and subsequently at 25 °C for six weeks prior to any experiments.

The thermograms were recorded on a VP-DSC microcalorimeter (MicroCal, Northampton, MA) using a heating rate of 20 °C/h. The reference and sample cells were filled with deionized water, and then the capillary tube was inserted in the sample cell. Excess water around the cell opening was carefully wiped out. The data acquisition and treatment were performed with the Origin software (Microcal software, Northampton, MA).

### 2.2. FT-IR spectroscopy

The homogeneous freeze-dried lipid mixture was hydrated with a large excess of the MES buffer (100 mM MES, 100 mM NaCl, and 5 mM EDTA), made in $D_2O$, at pD 5.6. $D_2O$ was used to avoid the spectral interference from the $H_2O$ deformation band, overlapping with the CO stretching mode of the carboxylic acid group and the Amide I band of the ceramide. For IR spectroscopy experiments, PA was substituted by its deuterated form (PA-$d_{31}$) so the alkyl chain order of ceramide and of the fatty acid could be simultaneously and independently characterized from the analysis of the $CH_2$ symmetric stretching ($\nu_{CH}$), and the $CD_2$ symmetric stretching ($\nu_{CD}$) band, respectively [30–34]. The final overall lipid concentration was about 10 mg/ml. The lipids were hydrated using an equilibration protocol similar to that used for the DSC experiments. The equilibration of the samples was validated by the appearance of the splitting of the $\delta CH_2$ and $\delta CD_2$ band, and by the Amide I′ band shape (see the Results section for a detailed discussion of these bands). The 40 °C incubation was necessary to obtain the maximum splitting of the $\delta CH_2$ band and the characteristic two-component Amide I′ band. During this period, PA-$d_{31}$ crystalline domains were partially destabilized, as assessed by the appearance of a component at 1089 $cm^{-1}$ in the $\delta CD_2$ region. A subsequent incubation at 25 °C led to the re-crystallization of PA-$d_{31}$ with an orthorhombic chain packing, without affecting the ceramide bands in the spectra. After the sample incubation, waxy lipid particles could be observed on the tube wall in a clear supernatant. For samples containing EtOH, a premixed EtOH/buffer solution was used for the lipid solvatation. The EtOH contents describe the composition of the solution for the sample equilibration; these likely decrease slightly during the course of data collection due to EtOH evaporation.

For the data acquisition, some waxy particles covered with a drop of buffer were squeezed in between two $CaF_2$ or $BaF_2$ windows separated by a 5 μm-thick Teflon spacer. For each spectrum, 40 scans were co-added with a 2 $cm^{-1}$ resolution, and the spectra were recorded from low to high temperatures, with a temperature-equilibration period of 6 minutes at each temperature. The spectra were recorded on a BioRad FTS-25 spectrometer, and treated using GRAMS software (Galactic Industries Corporation). The positions reported here corresponded to the center of gravity of the top 5% of the band measured on the spectra without any correction for the EtOH contribution. The main C-H stretching peaks of EtOH appeared above 2900 $cm^{-1}$, affecting only slightly the determination of the position of the C-H symmetric stretching mode of the lipid methylene groups. When the contribution of EtOH bands was subtracted from the spectra of lipid mixtures solvated with 60% EtOH, the difference between the band position before and after the subtraction was found to be less than 0.2 $cm^{-1}$.

### 2.3. $^2H$ NMR

The procedure for weighing, freeze-thaw and hydrating the lipid mixtures used in the $^2H$ NMR experiments was similar to the procedure for the DSC and FT-IR. Due to the inherently low signal to noise ratio of $^2H$-NMR acquisition, each sample contained 200 mg of lipid, in which either PA or Cer was perdeuterated. After hydration, the samples were transferred to NMR sample tubes (Li-Chan Mechanical Company Ltd., Taiwan), and, to prevent buffer evaporation, the threads at the top of the tubes were wrapped with Teflon tape and the tubes were sealed with Parafilm. Each sample was incubated at 33 °C for two to three weeks, and then stored at 37 °C until the sample was fully equilibrated, typically an additional six weeks. The state of equilibration was determined by measuring the percentage of lipids in the solid phase using $^2H$-NMR. The sample was considered fully equilibrated when the percentage of solid phase was above 82% for PA-$d_{31}$ and near 90% for Cer16-$d_{31}$ consistent with our earlier findings [4]. Ethanol was added to the equilibrated sample to obtain the desired proportion.

$^2H$-NMR spectra were acquired using a quadrupolar echo acquisition sequence [35] with a 3.95-μs 90° pulse and an interpulse delay of 40 μs. Spectra were recorded using a short repetition time (reptime) of 300 ms. In cases where slow-relaxing solid components were present, a long reptime, set to five times the $T_1$ of the component with the slowest relaxation, was used to collect spectra representative of the whole sample. For solid PA-$d_{31}$, the long reptime was 50 s, and for Cer16-$d_{31}$ it was 30 s. Spectra were acquired as a function of increasing temperature, from 25 to 62 °C: typically two short reptime spectra of 10 000 averages sandwiched a long reptime acquisition of 1000 averages.

From the short- and long-reptime spectra, it is possible to determine the distribution of the deuterated species in the different phases. We calculated the percentage of the deuterated lipid (PA-$d_{31}$ or Cer16-$d_{31}$) existing in a solid (%solid), an isotropic (%iso), and a fluid lamellar (%fluid) phase according to methods previously described [4]. The average spectral width ($M_1$) [36] was also calculated as a function of temperature and of EtOH content.

## 3. Results

### 3.1. DSC

In the absence of EtOH, the ternary Cer16/PA/chol mixture gave rise to three broad peaks in its thermogram (Fig. 1a). The peak maxima appeared at 47, 53, and 70 °C. The broad and asymmetric nature of the peaks is associated with the thermal evolution of the progressive mixing of the three lipids. This thermogram was reminiscent of those obtained previously from SC lipids[11,37–39]. On the basis of a previous study [4], the first endotherm of the thermogram that include the first two maxima (the heat absorption between 40, and 55 °C) is associated with a transition from solid lipids to a liquid ordered (lo) phase involving large proportions of PA-$d_{31}$ and cholesterol, and a smaller proportion of Cer16. The subsequent endotherm (55–75 °C) is associated with the progressive solubilization of Cer16 into the lo phase, which eventually leads to the destabilization of the lamellar phase at higher temperatures. The three observed maxima shifted toward lower temperatures in the presence of EtOH and the magnitude of this shift increased as a function of EtOH concentration. For the sample containing 60% EtOH, the maxima appeared at 35, 43, and 58 °C respectively. The second peak (with a maximum at 43 °C) almost disappeared whereas the amplitude of the last component (with a maximum at 58 °C) increased considerably. The influence of EtOH on the enthalpy variations determined from the thermograms is represented in Fig. 1b. In the absence of EtOH, the enthalpy variation of the first endotherm (40–55 °C) corresponded to 67 ± 3 J/g whereas that of the second endotherm (55–75 °C) was 42 ± 6 J/g. As the EtOH concentration in the solvating solution increased, the ΔH of the first endotherm progressively decreased while that of second increased. For the sample containing 60% EtOH, the ΔH reached 54 ± 1 and 73 ± 10 J/g for the first and the second endotherm respectively.

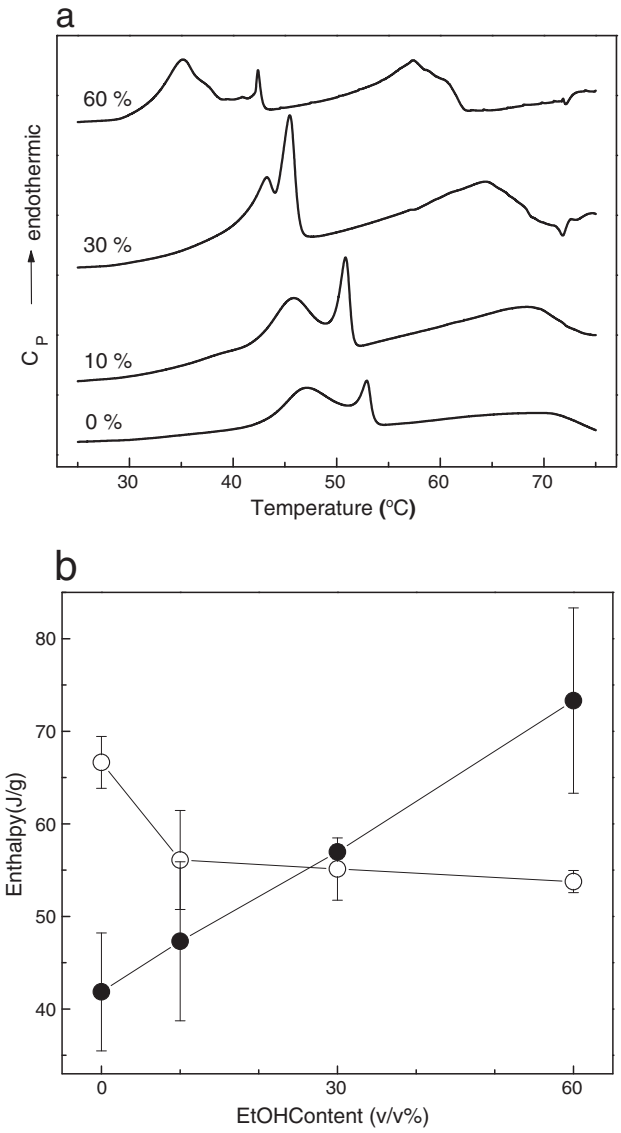


**Fig. 1.** a) Thermograms of equimolar Cer16/PA/Chol mixtures in the absence and in the presence of various amount of EtOH. The (v/v)% is indicated on the left of each trace. b) Effect of EtOH on the transition enthalpy of the equimolar Cer/PA/Chol mixtures. As described in the text, the enthalpies are reported for (○) the endothermic signals between 40, and 55 °C, shifting progressively towards lower temperature upon EtOH addition, and (●) for the broad endotherms at higher temperature, whose maximum is found between 70, and 58 °C, depending on the EtOH content. The reported values and their uncertainties correspond to the averages and the standard deviations calculated for n = 2.

### 3.2. IR spectroscopy

Fig. 2a shows the thermal behavior of the Cer16 in the model mixtures as probed by the position of the $\nu_{CH}$ band. Variations of the $\nu_{CH}$ band position are mainly associated with changes in the conformational order of Cer16 chains [31,32]. Between 25 and 40 °C, the $\nu_{CH}$ band was located below 2850 $cm^{-1}$ for all systems, indicating that most acyl chains were highly ordered over this temperature range [30,40]. Upon heating, the band shifted toward higher wave number, an indication of the disordering of the Cer16 chains. In the absence of

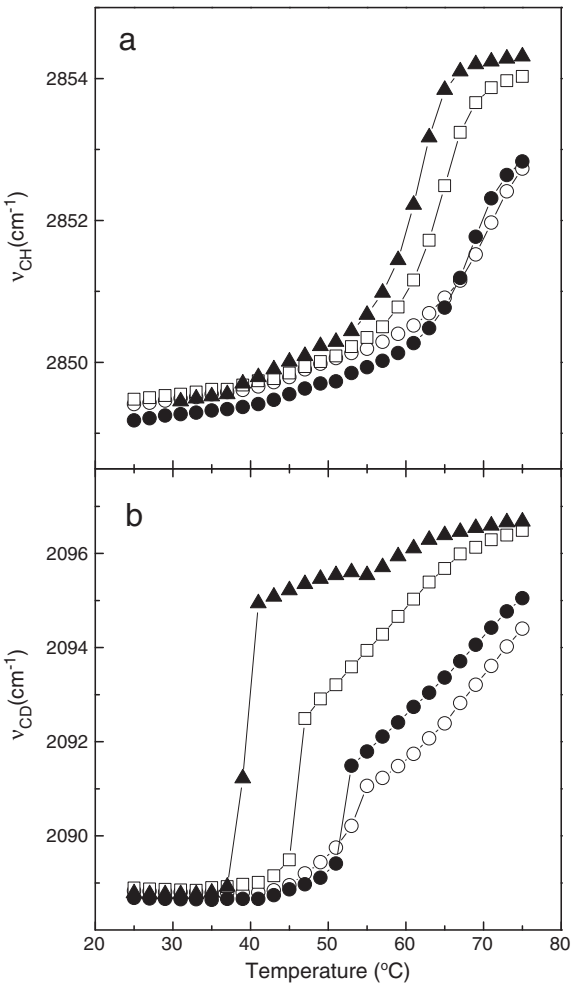


**Fig. 2.** Effect of EtOH on the thermal evolution of the acyl chain order of the equimolar Cer16/PA-$d_{31}$/Chol mixtures as probed by (a) the $\nu_{CH}$ band position and (b) $\nu_{CD}$ band position. (○) Lipid mixture hydrated with buffer free of EtOH, and containing (●) 10, (□) 30, and (▲) 60% of EtOH.

EtOH, as previously described [4], the $\nu_{CH}$ band showed a small shift toward higher wave number between 40 and 60 °C to reach ~2850 cm$^{-1}$, indicating that most of the ceramide chains were still ordered. Centered at ~68 °C, a rather abrupt shift to ~2853 cm$^{-1}$ suggested a melting of the solid ceramide to a disordered phase. No significant change was observed in the thermal behavior of the $\nu_{CH}$ band in the presence of 10% EtOH in the system. When 30 and 60% EtOH were added to the samples, EtOH promoted the disordering of ceramide alkyl chains mainly by decreasing the temperature of the ordered-disordered transition; this was shifted down to 60 °C in the case of the sample with 60% EtOH. The $\nu_{CH}$ band reached a plateau at ~2854 cm$^{-1}$ for 30 and 60% EtOH samples, indicating that the final state of ceramides corresponded to a fluid disordered phase. Only a slight increase of the $\nu_{CH}$ wave number was observed below 50 °C.

Fig. 2b shows the evolution of the $\nu_{CD}$ band position, probing the PA-$d_{31}$ chain order, as a function of temperature. Below 35 °C, the frequency of the band was lower than 2090 cm$^{-1}$ for all systems, indicating ordered acyl chains [30,33,34]. Upon heating, the $\nu_{CD}$ band shifted toward higher wave number, an indication of the disordering of the alkyl chains. In the absence of EtOH, the $\nu_{CD}$ band showed an initial shift at ~50 °C to ~2092 cm$^{-1}$, corresponding to the transition towards an lo phase as previously described [4], followed by a gradual shift to ~2095 cm$^{-1}$, indicating the further disordering of PA-$d_{31}$ alkyl chains. The PA-$d_{31}$ thermotropism in the ternary mixture was only slightly affected by the addition of 10% EtOH in the solvating buffer. The amplitude of the initial shift to ~2092 cm$^{-1}$ was more pronounced and the band position remained at a slightly higher wave number than those measured for the sample without EtOH. As the EtOH concentration increased, the first transition shifted dramatically towards lower temperatures and the band position subsequently reached high frequencies. For the 60% EtOH sample, the first increase of $\nu_{CD}$ appeared at 39 °C, downshifted by more than 15 °C compared to the EtOH-free lipid mixture. The band position shifted abruptly from 2089 to ~2096 cm$^{-1}$, suggesting a direct solid-disordered phase transition.

For the solvated lipid mixture incubated overnight in 80 (v/v) % EtOH solution, the IR spectrum of the waxy particles showed very weak PA-$d_{31}$ bands (data not shown), indicating the massive extraction of PA-$d_{31}$ from the waxy particles into the EtOH/water solution. This finding led us to directly quantify the PA-$d_{31}$ extraction from the various mixtures (Fig. 3). The PA-$d_{31}$ extraction was described by the ratio of the CD area ($A_{CD}$) over the sum of $A_{CD}$ and the CH area corrected for the EtOH contribution ($A_{CH}$): $A_{CD}/(A_{CD}+A_{CH})$. At 25 °C, this ratio was ~0.16 for the samples solvated with 0 and 10% EtOH solution whereas decreased to ~0.14 and ~0.11 for 30% and 60% EtOH solutions respectively. These ratios indicate that PA-$d_{31}$ was extracted from the solid lipid particles by the EtOH solution during the solvation of the lipid assemblies.

Lipid chain packing and compositional segregation was investigated using the $CD_2$ deformation ($\delta CD_2$) and $CH_2$ deformation ($\delta CH_2$) bands. The $\delta CD_2$ band was split for all the lipid mixtures at low temperature, giving rise to two components at ~1086 and ~1092 cm$^{-1}$ (data not shown). Because the splitting is due to interchain coupling, its presence indicated that the PA-$d_{31}$ in this mixture formed crystalline domains with an orthorhombic chain packing, composed almost exclusively of PA-$d_{31}$ [41–44]. The domains must include at least 100 molecules since the splitting was similar to that obtained with pure PA-$d_{31}$. The splitting remained unchanged in the presence of EtOH (up to 60 v/v %), even after incubations up to two weeks. These results suggest that, even though EtOH extracted some PA-$d_{31}$ molecules, it did not alter the structure of the remaining crystalline PA-$d_{31}$ domains. Upon heating, a peak at ~1089 cm$^{-1}$ grew while the intensity of the two peaks at ~1086 and ~1092 cm$^{-1}$ decreased. Moreover the splitting became smaller, indicating a decrease of the size and/or the PA-$d_{31}$ content of the orthorhombic crystalline domains. Eventually the $\delta CD_2$ deformation region was dominated by a broad band centered at ~1089 cm$^{-1}$. This region was analyzed following the method described elsewhere [45]; the three major peaks were curve-fitted and the intensity of the middle peak ($I_M$) was divided

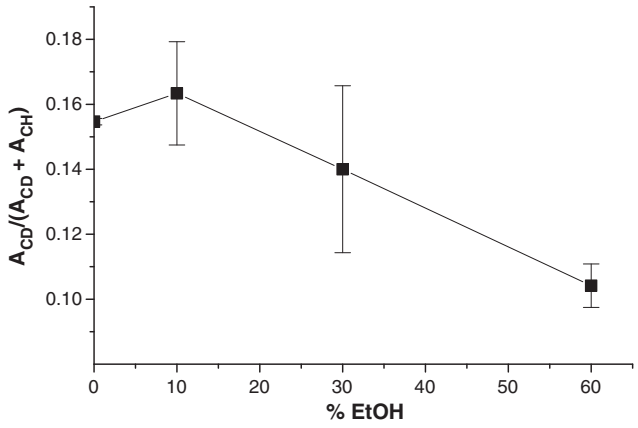


**Fig. 3.** Variations of the relative band area associated with the PA-$d_{31}$ chain C–D stretching as a function of the EtOH content — the decrease of the area corresponds to a relative extraction of PA-$d_{31}$ by EtOH from the SC model mixture. The reported values and their uncertainties correspond to the averages and the standard deviations calculated for n = 2.

by the total intensity of the whole multicomponent band ($I_T$). Fig. 4 shows the variation of the $I_M/I_T$ ratio as a function of temperature. The loss of the crystallinity with orthorhombic symmetry could be determined by the increase of the $I_M/I_T$ ratio and the complete loss of orthorhombic crystalline phase was obtained when the ratio became unity. In the absence of EtOH, the ratio began to increase at 43 °C and became 1 at 55 °C. The presence of EtOH promoted the disappearance of the PA-$d_{31}$ crystalline domains as the band splitting disappeared at lower temperatures. For the samples solvated with 10, 30, and 60% EtOH solutions, the two components merged completely at 53, 47, and 41 °C respectively, in a consistent manner with the $\nu_{CD}$ band behavior.

The $CH_2$ deformation ($\delta CH_2$) band also showed splitting at low temperature, indicating that ceramides were also in an orthorhombic crystalline phase (data not shown). The splitting was similar to that previously observed for pure ceramide [46]. Because the $\delta CH_2$ band overlaps with the contributions from the $\delta CH_2$ band of cholesterol and EtOH, and the Amide II′ band of Cer16, the splitting components were not as well resolved as in the case of the $\delta CD_2$ band and it was practically impossible to implement a curve-fitting method. A rather simple band analysis was therefore adopted: a linear baseline was drawn between 1458, and 1478 $cm^{-1}$ and the width of the band at 70% of its height from the baseline was measured as a function of temperature. The decrease in band width upon heating was mainly due to the collapse of the $\delta CH_2$ band splitting and, consequently, to the loss of the crystalline structure with orthorhombic chain packing (Fig. 5a). The temperature-induced narrowing was not constant over the whole investigated range as shown by the first derivatives of the width variation (Fig. 5b). In the absence of EtOH, the crystalline phase disappeared between 35 and 55 °C, as seen by the sharper narrowing of the $\delta CH_2$ band. This transition, also detected by a $\nu_{CH}$ band shift, is consistent with the previously reported solid-solid transition from an orthorhombic to a hexagonal chain packing [33,47]. The presence of EtOH had two effects on the $\delta CH_2$ width variations. First, the sharp decrease in width, observed as a minimum on the first derivative curves, occurred progressively at lower temperatures as the EtOH concentration increased up to 30 (v/v) %. For the 30% EtOH sample, the decrease of the $\delta CH_2$ width occurred between 30 and 45 °C. Second, in the presence of EtOH, another abrupt narrowing of the band was observed at 50–65 °C, highlighted by a second minimum in the first derivatives. The latter contribution dominated when the samples were equilibrated with 60% EtOH. The $\delta CH_2$ and $\delta CD_2$ splitting collapses for the 0, 10% and 30% EtOH samples were obtained over the same temperature ranges, between 30 and 55 °C. These coincident temperature ranges suggested that ceramide and PA-$d_{31}$ lost their orthorhombic crystallinity in a concerted manner for the lipid mixtures with moderate EtOH content or no EtOH. However, for the 60% EtOH sample, the $\delta CD_2$ splitting collapsed at much lower temperature than that of $\delta CH_2$, a discrepancy associated with the modification of the lipid composition as a consequence of the PA-$d_{31}$ solubilization by EtOH.

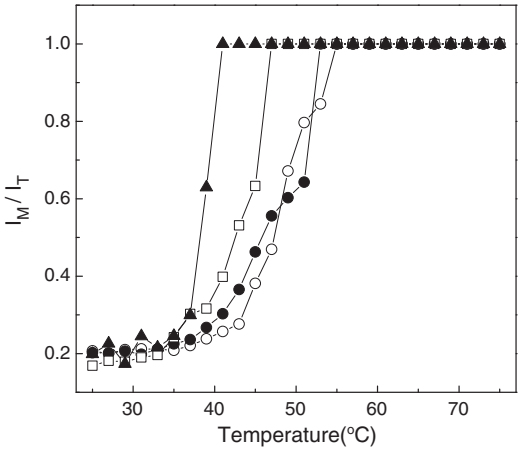


**Fig. 4.** Effect of EtOH on the thermal evolution of the orthorhombic chain packing of PA-$d_{31}$ in the equimolar Cer16/PA-$d_{31}$/Chol mixtures as described by the $CD_2$ deformation mode. (○) Lipid mixture hydrated with buffer free of EtOH, and containing (●) 10, (□) 30, and (▲) 60% of EtOH.

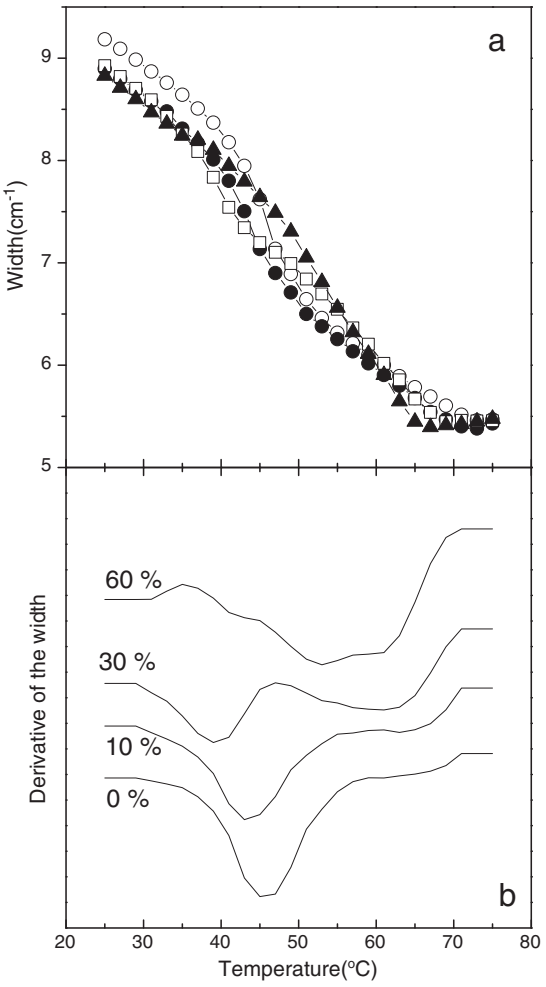


**Fig. 5.** Effect of EtOH on the thermal evolution of the orthorhombic chain packing of Cer16 in the equimolar Cer16/PA-$d_{31}$/Chol mixtures as described by the $CH_2$ deformation mode. a) Variation of the width of the $\delta CH_2$ mode, measured at 95% of the height of the peak. (○) Lipid mixture hydrated with buffer free of EtOH, and containing (●) 10, (□) 30, and (▲) 60% of EtOH. b) First derivative of the width of the $\delta CH_2$ mode relative to the temperature. The EtOH content in the solvating milieu is indicated next to each curve.

### 3.3. $^2H$ NMR

$^2H$-NMR of Cer16/PA/chol equimolar mixtures was performed on pair mixtures made with deuterated PA or deuterated ceramide. This approach allowed us to characterize the individual phase behavior of these two lipid species in the mixtures. Typical spectra presented in Fig. 6 show that they are valuable for phase identification. The spectra of the mixture in the absence of EtOH have been described elsewhere [4]. Briefly, at 25 °C, the spectra of both Cer16-$d_{31}$ and PA-$d_{31}$ in the equimolar Cer16/PA/chol mixtures displayed profiles typical of solid alkyl chain. Each spectrum was composed of two powder patterns with quadrupolar splittings (measured between the maxima for the 90° orientation) of about 120 and 35 kHz, assigned to the methylenes and the terminal methyl respectively. The peaks in the spectrum of Cer16-$d_{31}$ were not as sharp as in the

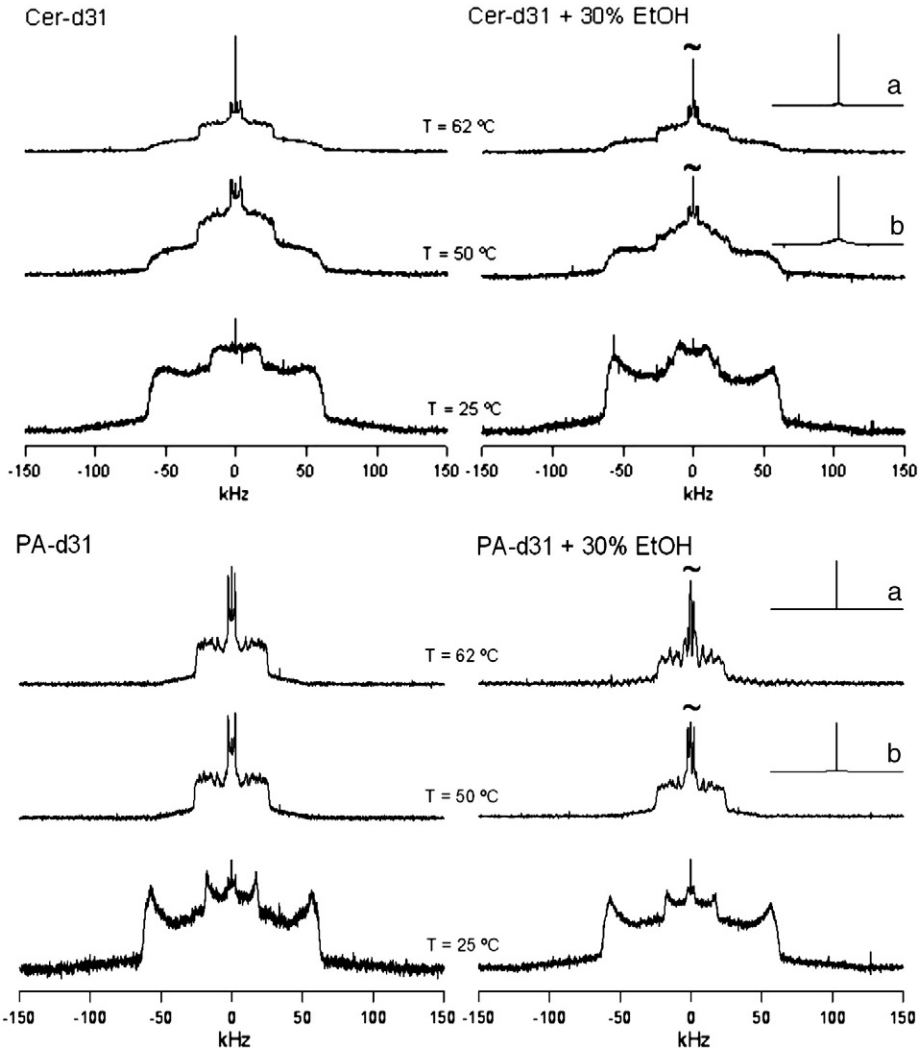


**Fig. 6.** $^2$H NMR spectra of Cer16/PA/chol equimolar mixture without EtOH (left), and containing 30% EtOH (right). The top row spectra were obtained with a mixture containing Cer16-$d_{31}$ whereas the bottom row spectra were obtained from the mirror mixture containing PA-$d_{31}$. The narrow lines present in the spectra with EtOH recorded at 50, and 62 °C were truncated; the full spectra, dominated by this line, are reproduced in the inserts.

case of the deuterated fatty acid, an observation that may be associated with slightly more mobility in the Cer16-$d_{31}$ chains since their attachment to the sphingosine backbone precludes such close chain-chain packing. At 50 °C, the spectra showed several overlapping powder patterns where the largest quadrupolar splitting corresponded to about 55 kHz, a signal characteristic of an lo phase [48–50]. The spectrum of the Cer16/PA-$d_{31}$/chol mixtures showed exclusively this lo signal whereas that of the mixture containing Cer16-$d_{31}$ was a co-existence of the lo signal and that of the solid lipid - about 60% of the ceramide molecules were in the solid phase. Upon further heating (see 62 °C), the spectra included a small narrow line, associated with a phase composed of lipids undergoing isotropic motions on the NMR time scale. Therefore, in the Cer16/PA/chol equimolar mixtures, the lipid molecules experience a transition from a solid-to-lo phase and then a lo-to-isotropic phase, the ceramide involvement in the lo phase being more limited at 50 °C. The main impact of the presence of 30% EtOH on the $^2$H NMR spectra of the mixture was the considerable increase of the contribution of the narrow line for both PA-$d_{31}$, and Cer16-$d_{31}$ at 50 and 62 °C. These spectra still included lamellar components as shown by the expansions in Fig. 6, and these underlying components are similar to those observed in the absence of EtOH.

In order to provide a more detailed picture of the thermal evolution of the phase composition, the first moments (M1) of the $^2$H-NMR spectra were plotted as a function of temperature (Fig. 7). A reduction in M1 implies that the labelled lipid is experiencing faster and/or more extreme motion, and a sudden change in M1 is usually associated with a change in lipid phase. In the case of Cer16-$d_{31}$, M1 was typical of solid phase between 25 and 45 °C for all EtOH concentrations. In the absence of EtOH, a decrease of M1 by about 20% was observed at ~50 °C. Upon further heating, the M1 values were relatively stable between 50 and 65 °C, and then decreased progressively. In the pair mixture made with PA-$d_{31}$, M1 had similar values between 25 and 45 °C and then dropped abruptly. The amplitude of this drop was significantly larger for PA-$d_{31}$ than for Cer16-$d_{31}$ as M1 values decreased by more than 50%. M1 was then roughly constant between 47 and 65 °C. Heating above 65 °C led to a progressive decrease of M1.

The influence of the presence of EtOH on M1 variations for the SC model mixtures is also shown in Fig. 7. For 10 and 30% EtOH, M1 was not affected at low temperature. The M1 variations for the Cer16-$d_{31}$/PA/chol mixture were similar to that obtained for the EtOH-free mixture. When the EtOH content was 71%, the ceramide disordering was shifted towards lower temperatures. The initial decrease was shifted from 50 to 40 °C, and this diminution was followed by a much more abrupt decrease of M1, reaching small values at ~60 °C, associated with the growing narrow central peak. For Cer16/PA-$d_{31}$/chol mixtures solvated with 10 or 30% EtOH, the M1 values were identical up to 40 °C. Subsequently, there was a decrease at ~45 °C that appeared to be slightly shifted towards low temperatures in the

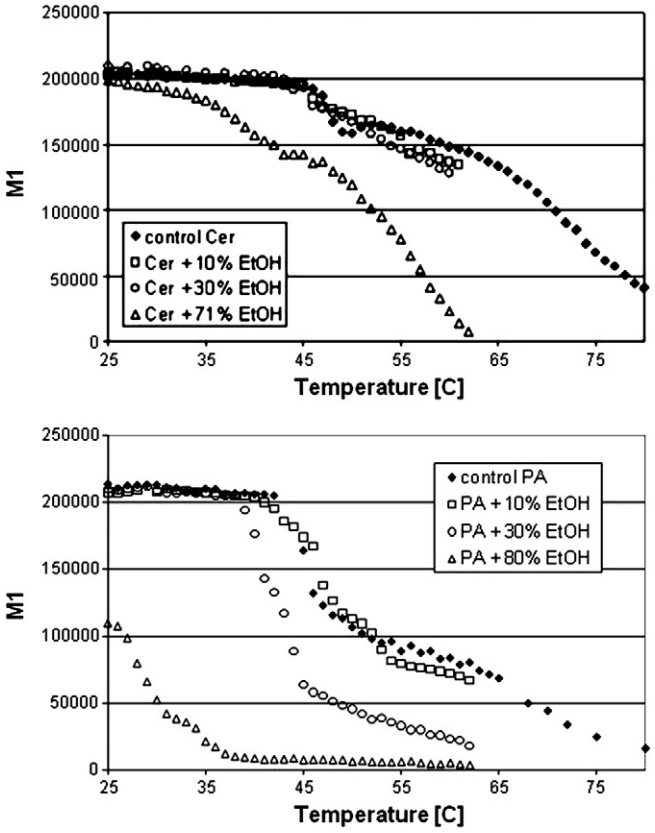


**Fig. 7.** Influence of EtOH on the thermal evolution of first moments calculated from the $^2$H-NMR spectra of Cer16/PA/chol equimolar mixture. The moments were obtained from the spectra of the mixtures containing Cer16-$d_{31}$ (top) and containing PA-$d_{31}$ (bottom). The variations of M1 were obtained for the SC model mixture (♦) hydrated with buffer free of EtOH, and containing (□) 10, (○) 30, and (△) 71-80% of EtOH.

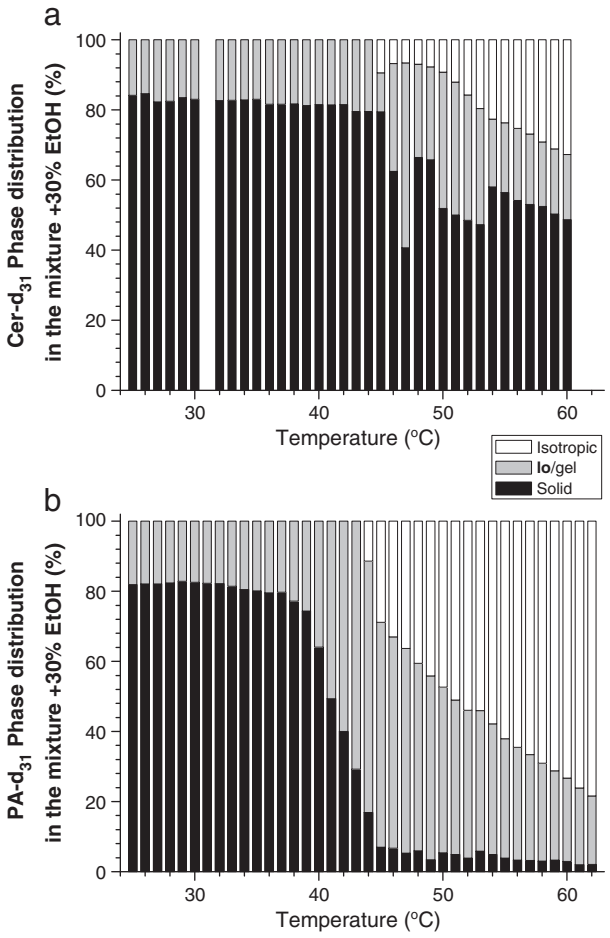


**Fig. 8.** Quantitative description of the phase composition as a function of temperature for the Cer16/PA/chol equimolar mixture in the presence of 30% EtOH. (a) describes the phase distribution of the Cer16-$d_{31}$ in the sample whereas (b) describes the phase distribution of PA-$d_{31}$.

presence of EtOH. Between 45 and 65 °C, M1 was systematically lower in the presence of 30% EtOH and a progressive reduction in M1 contrasted with the plateau obtained for EtOH-free mixture. When the samples contained 80% EtOH, the value of M1 were drastically reduced. Even at 25 °C, M1 was reduced by ~50% relative to that measured in the absence of EtOH. The values decreased continuously reaching, near 35 °C, values associated with a predominant narrow line in the spectrum. Note that in contrast to the IR peak intensity measurements, reductions in M1 do not imply a reduction in the amount of labelled lipid in the sample; in the NMR experiment, any extracted deuterium-labelled lipid will contribute signal to the isotropic central peak.

The spectra were analyzed according to a procedure described elsewhere [4] that allowed us to quantify the proportions of the existing phases in the samples. This analysis was carried out for both Cer16 and PA and the results are summarized in Fig. 8 for the Cer16/PA/chol mixture solvated with 30% EtOH. The results obtained for the SC model mixture in the absence of EtOH have been already reported [4]. In that EtOH-free mixture, most of the lipids were in the solid phase below 40 °C. It should be pointed out that about 10–20% of the lipids were in the lo phase, a behavior that was also observed in other SC model mixtures [51]. Between 40 and 45 °C, most of the fatty acid (~90%) melted from the solid to the lo phase whereas only ~30% of the Cer16 was involved in this transition. Above 55 °C, Cer16 and PA underwent a transition towards an isotropic phase. At 60 °C less than 10% of the lipids were in this phase. The proportion of this isotropic phase at 80 °C corresponded to 50 and 75% for Cer16 and PA respectively.

The presence of 30% EtOH led to two main changes in this phase behavior. First, the solid-to-lo phase transition experienced mainly by PA was downshifted by a few degrees, as already illustrated by the M1 variations. Second, the alcohol promoted the formation of the isotropic phase for both PA and Cer16. At 60 °C, the proportion of lipid involved in this phase was 30 and 70% for Cer16 and PA respectively.

## 4. Discussion

Ethanol affects phase behavior of our lipid model membranes. The observed effects are concentration dependent (although apparently non-linear) and are most marked on the palmitic acid component. No significant effect was observed when the aqueous dispersing phase contained 10% EtOH (vol/vol). A dispersing medium of 30%-EtOH content significantly perturbed the temperature dependent phase behavior of the lipid mixture: at 30 °C, the individual lipid components remained in the crystalline/solid form but the temperature of the solid-lo phase transition that involves mainly PA and cholesterol was reduced by 5–10 °C. Between 40 and 45 °C, an extensive fluidification of PA that also very likely involves cholesterol is induced while Cer16 remains predominantly in a solid form; this phenomenon is particularly explicit in Fig. 8. Under these conditions, EtOH acts as a fluidizer of the SC lipid bilayers but the present results indicate that this statement is essentially based on its effect on the fatty acid component. The disordering impact of EtOH also manifests at higher temperatures as the formation of an isotropic phase is promoted. It should be pointed out that, even though this transition appears to be driven by PA, it also includes the disordering of some Cer16.

When the EtOH content reaches 60%, the changes in lipid phase behaviour are more marked compared to the controls without ethanol and define another regime. At this concentration, EtOH extracts PA from the solid lipid mixture (as shown by the relative C–D and C–H stretching band areas measured by IR spectroscopy), leading to the formation of a phase showing isotropic PA motions (as seen by the low M1 values measured by $^2$H NMR). The remaining PA still adopts a solid phase with orthorhombic chain packing below 35 °C but its transition towards a disordered phase is shifted, as observed by DSC, IR, and $^2$H NMR spectroscopy, from ~50 to ~37 °C when 60% EtOH is present in the solvating milieu. In terms of fluidification and extraction, the presence of EtOH affects PA the most significantly. In parallel, Cer16 is affected but to a lesser extent: this species remains practically all solid at room temperature but undergoes a chain disordering process starting at 35 °C that becomes accentuated at 55 °C, as highlighted by the increase of the contribution of second endotherm (55–75 °C) in the thermograms, the abrupt upshift of the $\nu_{CH}$ band in the IR spectra, as well as the sharp decrease of M1 of the $^2$H NMR spectra of the samples containing Cer16-$d_{31}$. Therefore, 60% EtOH can lead to their extensive heat-induced disordering; this disorder is rather unusual for Cer16 which has a melting point of 93 °C [52]. We conclude that in these model systems, the palmitic acid is more susceptible to ethanol than is ceramide both in terms of reduction of transition temperatures to more disordered phases and lipid extraction.

We are aware of the differences between the model membranes we have used and native stratum corneum intercellular membranes. First, there is more chain length asymmetry in native ceramides and fatty acids, and less “hydrophobic matching” than is the case for the models reported here. This simplification appears to lead to a more extensive phase separation compared to mixtures with heterogeneous alkyl chain lengths [4,53]. Second, there is “long range order” in native SC intercellular membranes, and in particular a 13 nm repeat lamellar structure that is not replicated in our models. Third, the free fatty acid composition of mammalian and particularly human SC inter cellular membranes is longer than the C16 used here, and typically varies from C18 to C24. Finally, our samples are prepared by dispersion of lipids freeze dried from organic solvents in defined aqueous media, freeze/thawed and equilibrated for long periods (days or weeks) before measurement. The process of *in vivo* crystallization must occur differently. All of these differences might well result in solid “domains” that differ in structure and composition from those described in our models. Nevertheless, both the presence of crystalline lipid domains with orthorhombic chain packing and the thermotropism of the model mixture are analogous to the reported behaviour of natural SC lipids [5–10]. The intermolecular interactions that dictate the phase behavior of the model mixture are obviously also present when skin is exposed to EtOH and we believe that the observed interactions should be transferable to a large extent from model to natural SC.

Singer and Nicholson predicted the existence of “solid” biological membranes [54], and these have been found to exist in stratum corneum intercellular membranes. We believe that the extent and architecture of solid lipid domains within stratum corneum intercellular membranes are essential for the skin's permeability barrier, as previously hypothesized [55–57]. That such solid membranes might be in dynamic equilibrium with the external environment is also to be expected. Apart from the intrinsic interest in such unusual biological membranes, we believe there are obvious practical implications.

Our results lead us to propose that EtOH would act as a penetration enhancer by two mechanisms that are dependent on its concentration. First, EtOH acts as a fluidizer of SC solid lipid domains. This lipid disordering is essentially observed for EtOH content ≥ 30% and it is observable at 37 °C only with pure EtOH, as inferred by DSC and IR spectroscopy. The fluidification of the SC lipid matrix as a mechanism for penetration enhancement has been previously proposed [14,21]. In fact, a relationship between the effect of chemical enhancers on the position of the $\nu_{CH}$ band of SC lipids and their permeation enhancement was recently proposed [58]. The increase in vibration wave number is much more pronounced for the $\nu_{CD}$ than for the $\nu_{CH}$ mode demonstrating that, at least in our SC model, the fatty acid is more susceptible to EtOH disordering. The effect of EtOH on the $\nu_{CH}$ band of skin or SC has been reported in a few studies but no consensus can be inferred. A considerable increase (2852 $cm^{-1}$ or higher) of the mode wave number was reported for human skin in contact with EtOH [59] and for abdominal rat skin with 40–60% EtOH [21]. However, no considerable shift was reported when porcine SC was treated with an EtOH/water mixture (20 to 80%) or pure EtOH [24] and, conversely, a transient decrease of the $\nu_{CH}$ vibration was reported when human SC was treated with pure EtOH [60]. Our results favour the hypothesis that EtOH causes fluidification of the SC lipid matrix and fatty acids appear to be mainly affected. Second, we report that EtOH can achieve lipid extraction from our SC model mixture; this phenomenon is observed for large proportions of EtOH (≥30%). Such lipid extraction is actually consistent with several previous studies on the effect of EtOH on SC [17,19,21–24]. It was found that about 10% of lipids were extracted from SC when incubated in an aqueous solution with 40 or 50% EtOH [23,24]. Between 20 and 25% of lipids were extracted (as inferred from the intensity of the CH stretching region of the IR spectra) from human and rat SC when treated with a mixture of EtOH/water 60/40 [17,22]. With pure EtOH, lipid extractions of 28% and 55% were reported from pig abdominal [24] and ear [19] SC, respectively. Therefore the literature results appear to also follow the trend observed in our model mixture regarding the EtOH content and the extent of the lipid extraction. Our study specifies that free fatty acid is more susceptible to this extraction than ceramide. Even though no study, to our knowledge, has provided the speciation of the extracted lipid materials in the presence of EtOH, it should be noted that a previous study [24] indicated that the signal from the C=O stretching of the carboxylic group, essentially assigned to the fatty acids, was drastically reduced when the SC extracted from pig abdominal skin was immersed in pure EtOH. This observation on real SC reinforces our conclusion inferring the foremost participation of fatty acids in this process.

In addition to agents applied to stratum corneum to increase the permeability to drugs, human skin is now in contact with manufactured environments that might alter its barrier function. The obvious example is repeated exposure to detergent in hand washing, but a more recent use is alcohol-based “rubs” used particularly to disinfect hands, in which the ethanol or other alcohol concentration typically exceeds 60% . The effect of repeated exposures of ethanol and detergent on individual lipids of stratum corneum intercellular membranes is of interest with respect to barrier function (e.g. [61]).

## 5. Conclusion

We conclude that ethanol perturbs the phase behaviour of our model system, a lipid in water dispersion containing the three major classes of lipids found in SC intercellular membranes. There are two major effects: (1) the reduction of temperature for the transition from a “solid” lipid crystal (in which there is no rotational or lateral diffusion of lipids in the plane of the membrane) to a fluid bilayer more typical of most biological membranes, in proportion to the ethanol concentration of the solvent; and (2) selective extraction of the free fatty acid component from the ensemble, most evident at high ethanol concentration. Although our three component system is artificial, we speculate that ethanol applied to native SC will act both to increase the proportion of fluid rather

than solid intercellular lipid domains, and to selectively extract free fatty acids. These effects are consistent with the observed EtOH-induced increase in SC permeability to drugs, and conversely, its decrease in effectiveness as a barrier.

## Acknowledgements

The authors thank the Natural Sciences and Engineering Research Council of Canada for the financial support of this Collaborative Health Research Project. ML is also grateful to the Fond Québécois de la Recherche sur la Nature et les Technologies (FQRNT) for its financial support to the Center for Self-Assembled Chemical Systems (CSACS). JT thanks Carolyn Young for help with NMR data collection and analysis.

## References

[1] P.W. Wertz, Lipids and barrier function of the skin, Acta Derm. Venereol., Suppl. 208 (2000) 7–11.
[2] P.M. Elias, Epidermal lipids, barrier function, and desquamation, J. Invest. Dermatol. 80 (1983) 44s–49s.
[3] J. Hadgraft, Passive enhancement strategies in topical and transdermal drug delivery, Int. J. Pharm. 184 (1999) 1–6.
[4] E. Brief, S. Kwak, J.T.J. Cheng, N. Kitson, J. Thewalt, M. Lafleur, The phase behaviour of equimolar mixture of *N*-palmitoyl D-*erythro*-sphingosine, cholesterol and palmitic acid, a mixture with optimized hydrophobic matching, Langmuir 25 (2009) 7523–7532.
[5] D.T. Parrott, J.E. Turner, Mesophase formation by ceramides and cholesterol: a model for stratum corneum lipid packing? Biochim. Biophys. Acta 1147 (1993) 273–276.
[6] Y.-L. Chen, T.S. Wiedmann, Human stratum corneum lipids have a distorted orthorhombic packing at the surface of cohesive failure, J. Invest. Dermatol. 107 (1996) 15–19.
[7] J.A. Bouwstra, G.S. Gooris, W. Bras, D.T. Downing, Lipid organization in pig stratum corneum, J. Lipid Res. 36 (1995) 685–695.
[8] J.A. Bouwstra, G.S. Gooris, K. Cheng, A.M. Weerheim, W. Bras, M. Ponec, Phase behavior of isolated skin lipids, J. Lipid Res. 37 (1996) 999–1011.
[9] J.A. Bouwstra, G.S. Gooris, J.A. van der Spek, W. Bras, Structural Investigations of Human Stratum Corneum by Small-Angle X-ray Scattering, J. Invest. Dermatol. 97 (1991) 1005–1012.
[10] J.A. Bouwstra, G.S. Gooris, M.A. Salomons-de Vries, J.A. van der Spek, W. Bras, Structure of Human Stratum Corneum as a Function of Temperature and Hydratation: A Wide-angle X-Ray Diffraction Study, Int. J. Pharm. 84 (1992) 205–216.
[11] G.M. Golden, D.B. Guzek, R.R. Harris, J.E. Mckie, R.O. Potts, Lipid thermotropic transitions in human stratum corneum, J. Invest. Dermatol. 86 (1986) 255–259.
[12] R.O. Potts, M.L. Francoeur, Infrared spectroscopy of stratum corneum lipids, Drugs Pharm. Sci. 59 (1993) 269–291.
[13] B. Ongpipattanakul, M.L. Francoeur, R.O. Potts, Polymorphism in stratum corneum lipids, Biochim. Biophys. Acta 1190 (1994) 115–122.
[14] R. Panchagnula, P.S. Salve, N.S. Thomas, A.K. Jain, P. Ramarao, Transdermal delivery of naloxone: effect of water, propylene glycol, ethanol and their binary combinations on permeation through rat skin, Int. J. Pharm. 219 (2001) 95–105.
[15] N.A. Megrab, A.C. Williams, B.W. Barry, Oestradiol permeation across human skin, silastic and snake skin membranes: the effects of ethanol/water co-solvent systems, Int. J. Pharm. 116 (1995) 101–112.
[16] G.-S. Chen, D.-D. Kim, Y.W. Chien, Dual-controlled transdermal delivery of levonorgestrel and estradiol: enhanced permeation and modulated delivery, J. Control. Release 34 (1995) 129–143.
[17] T. Kurihara-Bergstrom, K. Knutson, L.J. DeNoble, C.Y. Goates, Percutaneous adsorption enhancement of an ionic molecule by ethanol-water systems in human skin, Pharm. Res. 7 (1990) 762–766.
[18] D.-D. Kim, J.L. Kim, Y.W. Chien, Mutual hairless rat skin permeation-enhancing effect of ethanol/water system and oleic acid, J. Pharm. Sci. 85 (1996) 1191–1195.
[19] A.K. Levang, K. Zhao, J. Singh, Effect of ethanol/propylene glycol on the in vitro percutaneous absorption of aspirin, biophysical changes and macroscopic barrier properties of the skin, Int. J. Pharm. 181 (1999) 255–263.
[20] D.-D. Kim, Y.W. Chien, Simultaneous skin permeation of dideoxynucleoside-type anti-HIV drugs, J. Control. Release 40 (1996) 67–76.
[21] E. Manabe, K. Sugibayashi, Y. Morimoto, Analysis of skin penetration enhancing effect of drugs by ethanol-water mixed systems with hydrodynamic pore theory, Int. J. Pharm. 129 (1996) 211–221.
[22] Y.S.R. Krishnaiah, P. Bhaskar, V. Satyanarayana, Penetration-enhancing effect of ethanol-water solvent system and ethanolic solution of carvone on transdermal permeability of nimodipine from HPMC gel across rat abdominal skin, Pharm. Dev. Technol. 9 (2004) 63–74.
[23] Y. Obata, Y. Maruyama, K. Takayama, The mode of promoting activity of O-ethylmenthol as a transdermal absoprion enhancer, Pharm. Res. 23 (2006) 392–400.
[24] D. Van der Merwe, J.E. Riviere, Comparative studies on the effects of water, ethanol and water/ethanol mixtures on chemical partitioning into porcine stratum corneum and silastic membrane, Toxicol. In Vitro 19 (2005) 69–77.
[25] C.M. Heard, C. Screen, Probing the permeation enhancement of mefenamic acid by ethanol across full-thickness skin, heat-separated epidermal membrane and heat-separated dermal membrane, Int. J. Pharm. 349 (2008) 323–325.
[26] C.M. Heard, D. Kung, C.P. Thomas, Skin penetration enhancement of mefenamic acid by ethanol and 1,8-cineole can be explained by the 'pull' effect, Int. J. Pharm. 321 (2006) 167–170.
[27] C.K. Lee, T. Uchida, E. Noguchi, N.-S. Kim, S. Goto, Skin permeation enhancement of tegafur by ethanol/panasate 800 or ethanol/water binary vehicle and combined effect of fatty acids and fatty alcohols, J. Pharm. Sci. 82 (1993) 1155–1159.
[28] C.Y.Y. Hsiao, C.A. Ottaway, D.B. Wetlaufer, Preparation of fully deuterated fatty acids by simple method, Lipids 9 (1974) 913–915.
[29] D.B. Fenske, J.L. Thewalt, M. Bloom, N. Kitson, Model of stratum corneum intercellular membranes: $^2$H NMR of macroscopically oriented multilayers, Biophys. J. 67 (1994) 1562–1573.
[30] M. Lafleur, Phase behaviour of model stratum corneum lipid mixtures: an infrared spectroscopy investigation, Can. J. Chem. 76 (1998) 1501–1511.
[31] V.R. Kodati, R. El-Jastimi, M. Lafleur, Contribution of the intermolecular coupling and librotorsional mobility in the methylene stretching modes in the infrared spectra of acyl chains, J. Phys. Chem. 98 (1994) 12191–12197.
[32] H.H. Mantsch, R.N. McElhaney, Phospholipid phase transitions in model and biological membranes as studied by infrared spectroscopy, Chem. Phys. Lipids 57 (1991) 213–226.
[33] H.-C. Chen, R. Mendelsohn, M.E. Rerek, D.J. Moore, Effect of cholesterol on miscibility and phase behavior in binary mixtures with synthetic ceramide 2 and octadecanoic acid. Infrared studies, Biochim. Biophys. Acta 1512 (2001) 345–356.
[34] J. Ouimet, M. Lafleur, Hydrophobic match between cholesterol and saturated fatty acid is required for the formation of lamellar liquid ordered phases, Langmuir 20 (2004) 7474–7481.
[35] J.H. Davis, K.R. Jeffrey, M. Bloom, M.I. Valic, T.P. Higgs, Quadrupolar echo deuteron magnetic resonance spectroscopy in ordered hydrocarbon chains, Chem. Phys. Lett. 42 (1976) 390–394.
[36] Y.W. Hsueh, R. Giles, N. Kitson, J. Thewalt, The effect of ceramide on phosphatidylcholine membranes: a deuterium nmr study, Biophys. J. 82 (2002) 3089–3095.
[37] R. Pouliot, L. Germain, F.A. Auger, N. Tremblay, J. Juhasz, Physical characterization of the stratum corneum of an in vitro human skin equivalent produced by tissue engineering and its comparison with normal human skin by ATR-FTIR spectroscopy and thermal analysis (DSC), Biochim. Biophys. Acta 1439 (1999) 341–352.
[38] C.L. Silva, S.C.C. Nunes, M.E.S. Eusébio, J.J.S. Sousa, A.A.C.C. Pais, Study of human stratum corneum and extracted lipids by thermomicroscopy and DSC, Chem. Phys. Lipids 140 (2006) 36–47.
[39] S.J. Rehfeld, W.Z. Plachy, M.L. Williams, P.M. Elias, Calorimetric and electron spin resonance examination of lipid phase transitions in human stratum corneum: molecular basis for normal cohesion and abnormal desquamation in recessive X-linked ichthyosis, J. Invest. Dermatol. 91 (1988) 499–505.
[40] D.J. Moore, M.E. Rerek, R. Mendelsohn, FTIR spectroscopy studies of the conformational order and phase behavior of ceramides, J. Chem. Phys. B 101 (1997) 8933–8940.
[41] R.G. Snyder, M.C. Goh, V.J.P. Srivatsavoy, H.L. Strauss, D.L. Dorset, Measurement of the growth kinetics of microdomains in binary n-alkane solid solutions by infrared spectroscopy, J. Phys. Chem. 96 (1992) 10008–10019.
[42] R.G. Snyder, V.J.P. Srivatsavoy, D.A. Cates, H.L. Strauss, J.W. White, D.L. Dorset, Hydrogen/deuterium isotope effects on microphase separation in unstable crystalline mixtures of binary n-alkanes, J. Phys. Chem. 98 (1994) 674–684.
[43] R.G. Snyder, H.L. Strauss, D.A. Cates, Detection and measurement of microaggregation in binary mixtures of esters and of phospholipid dispersions, J. Phys. Chem. 99 (1995) 8432–8439.
[44] D.J. Moore, R.G. Snyder, M.E. Rerek, R. Mendelsohn, Kinetics of membrane raft formation: fatty acid domains in stratum corneum lipid models, J. Chem. Phys. B 110 (2006) 2378–2386.
[45] X. Chen, S. Kwak, M. Lafleur, M. Bloom, K. Kitson, J. Thewalt, Fatty acids influence "solid" phase formation in models of stratum corneum intercellular membranes, Langmuir 23 (2007) 5548–5556.
[46] V. Velkova, M. Lafleur, Influence of the lipid composition on the organization of skin lipid model mixtures: an infrared spectroscopy investigation, Chem. Phys. Lipids 117 (2002) 63–74.
[47] H.-C. Chen, R. Mendelsohn, M.E. Rerek, D.J. Moore, Fourier transform infrared spectroscopy and differential scanning calorimetry studies of fatty acid homogeneous ceramide 2, Biochim. Biophys. Acta 1468 (2000) 293–303.
[48] M.R. Vist, J.H. Davis, Phase equilibria of cholesterol/dipalmitoylphosphatidylcholine mixtures: $^2$H nuclear magnetic resonance and differential scanning calorimetry, Biochemistry 29 (1990) 451–464.
[49] M. Lafleur, P.R. Cullis, M. Bloom, Modulation of the orientational order profile of the lipid acyl chain in the Lα phase, Eur. Biophys. J. 19 (1990) 55–62.
[50] C. Paré, M. Lafleur, Polymorphism of POPE/cholesterol system: a $^2$H nuclear magnetic resonance and infrared spectroscopic investigation, Biophys. J. 74 (1998) 899–909.
[51] N. Kitson, J. Thewalt, M. Lafleur, M. Bloom, A model membrane approach to the epidermal permeability barrier, Biochemistry 33 (1994) 6707–6715.

[52] J. Sot, F.J. Aranda, M.-I. Collado, F.M. Goñi, A. Alonso, Different effects of long- and short-chain ceramides on the gel-fluid and lamellar-hexagonal transitions of phospholipids: a calorimetric, NMR, and x-ray diffraction study, Biophys. J. 88 (2005) 3368–3380.
[53] M.W. de Jager, G.S. Gooris, I.P. Dolbnya, W. Bras, M. Ponec, J.A. Bouwstra, The phase behaviour of skin lipid mixtures based on synthetic ceramides, Chem. Phys. Lipids 124 (2003) 123–134.
[54] S.J. Singer, G.L. Nicolson, The fluid mosaic model of the structure of cell membranes, Science 175 (1972) 720–731.
[55] B. Forslind, A domain mosaic model of the skin barrier, Acta Derm. Venereol. 74 (1994) 1–6.
[56] B. Forslind, L. Norlén, J. Engblom, A structural model for the human skin barrier, Prog. Colloid Polym. Sci. 108 (1998) 40–46.
[57] N. Kitson, J.L. Thewalt, Hypothesis: the epidermal permeability barrier is a porous medium, Acta Derm. Venereol. Suppl. (Stockh.) 208 (2000) 12–15.
[58] S.A. Ibrahim, S.K. Li, Chemical enhancer solubility in human stratum corneum lipids and enhancer mechanism of action on stratum corneum lipid domain, Int. J. Pharm. 383 (2010) 89–98.
[59] C. Merle, A. Baillet-Guffroy, Physical and chemical perturbations of the supramolecular organization of the stratum corneum lipids: In vitro to ex vivo study, Biochim. Biophys. Acta 1788 (2009) 1092–1098.
[60] D. Bommannan, R.O. Potts, R.H. Guy, Examination of the effect of ethanol on human stratum corneum in vivo using infrared spectroscopy, J. Control. Release 16 (1991) 299–304.
[61] H. Löffler, G. Kampf, D. Schmermund, H. Maibach, How irritant is alcohol? Br. J. Dermatol. 157 (2007) 74–81.